Supplementary materials

Reduced Graphene Oxide/NiCoP Electrocatalysts via a Facile Synthetic Strategy for Efficient Hydrogen Evolution in Alkaline Media

Hui Ni[a], Zhen Ma[b], Jianyi Qin[a], Xin Zhang[a], Jing Zhang[a], Bin Zhao[a]*

[a]*School of Materials & Chemistry, University of Shanghai for Science and Technology, Shanghai 200093, China*
[b]*Edwards Technologies, Shanghai 201203, China*

Experimental

The two-electrode electrolyzer was assembled by using the rGO/NiCoP catalyst-coated carbon cloth (1 cm × 1.2 cm, with an exposed geometric area of 1 cm^2) as the cathode, and RuO_2 as the anode. The distance between the cathode and anode was approximately 2 cm, with 1 M KOH (pH = 14) serving as the electrolyte. No separator was used, and the electrolyte was not stirred during the measurements to maintain stable and reproducible conditions, with gas bubbles evolved during electrolysis allowed to detach naturally. The polarization curves for overall water splitting were recorded without iR compensation to reflect the actual cell voltage under operating conditions.

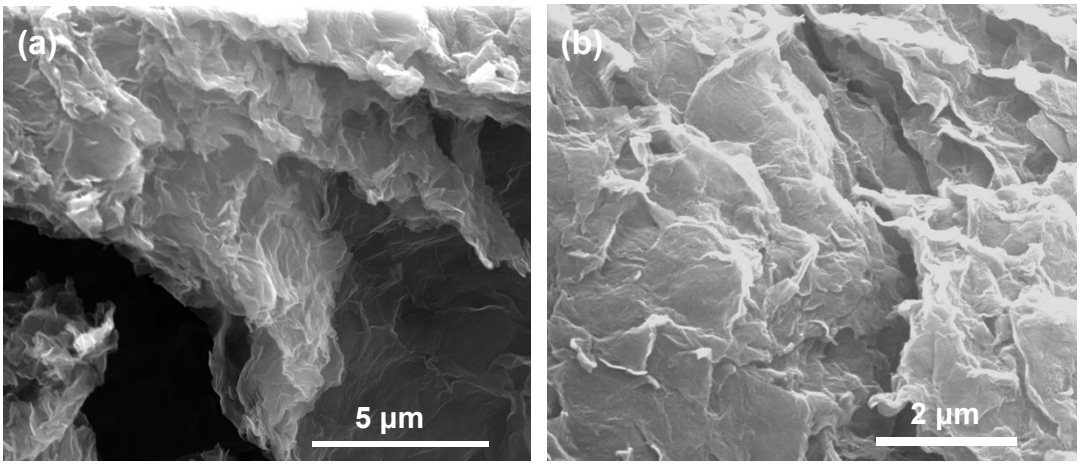

Fig. S1 SEM image of rGO/$NiCoO_2$.

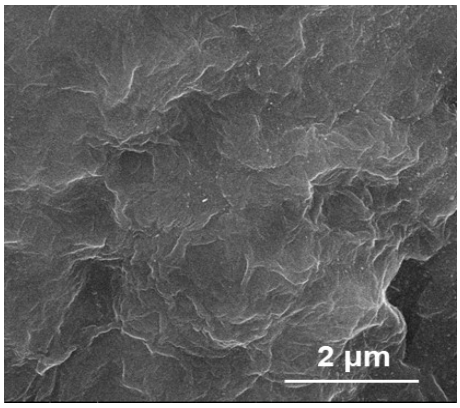

Fig. S2 SEM image of rGO/NiCoP.

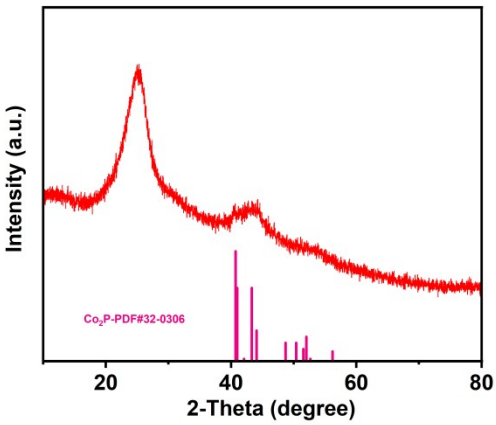

Fig. S3 XRD pattern of rGO/Co_2P.

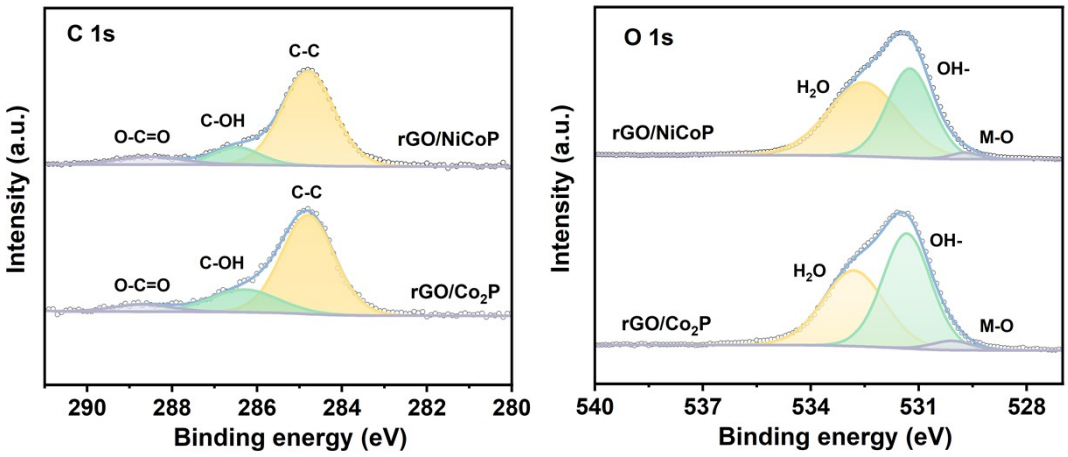

Fig. S4 XPS spectrum of C 1s (a) and O 1s (f) for rGO/NiCoP and rGO/Co_2P.

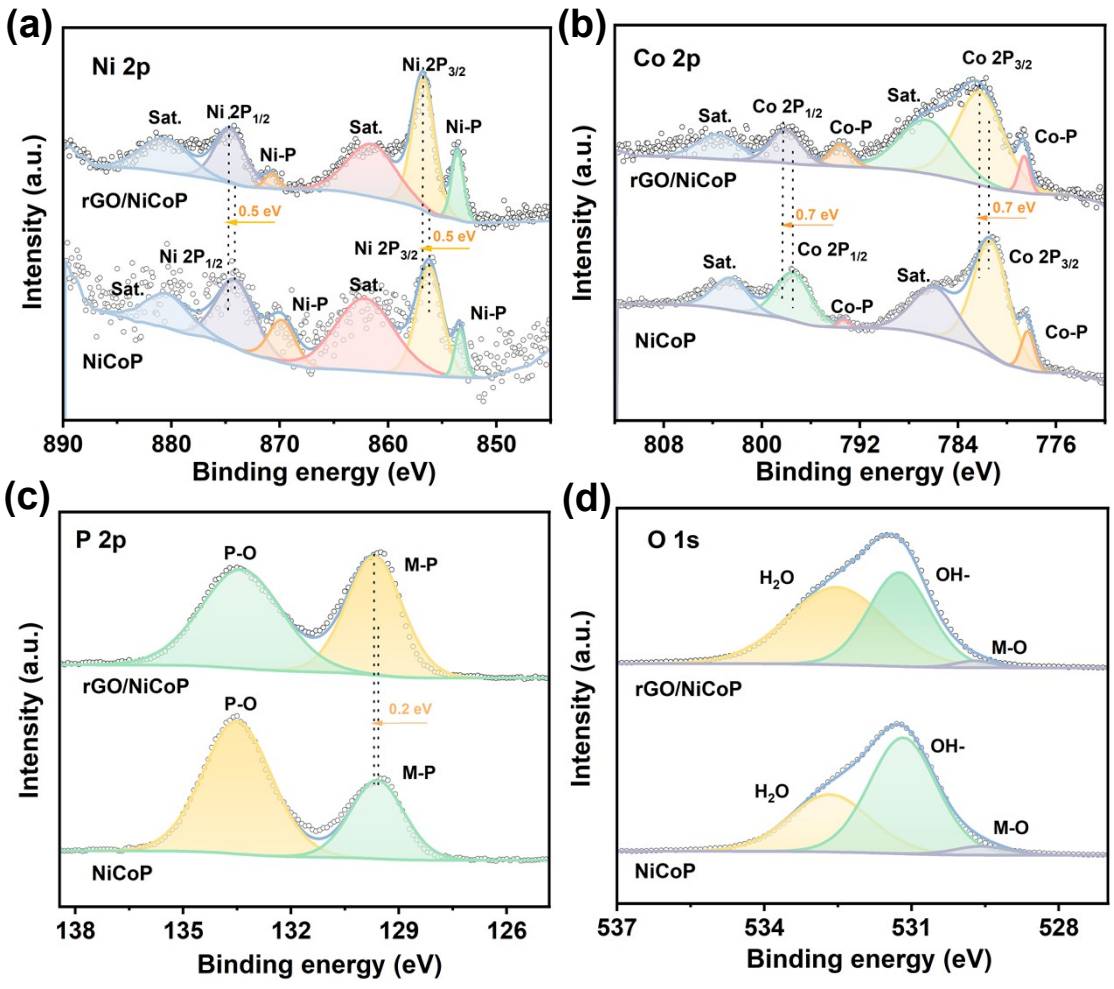

Fig. S5 XPS spectra of rGO/NiCoP and NiCoP (a) Ni 2p, (b) Co 2p, (c) P 2p, (d) O 1s.

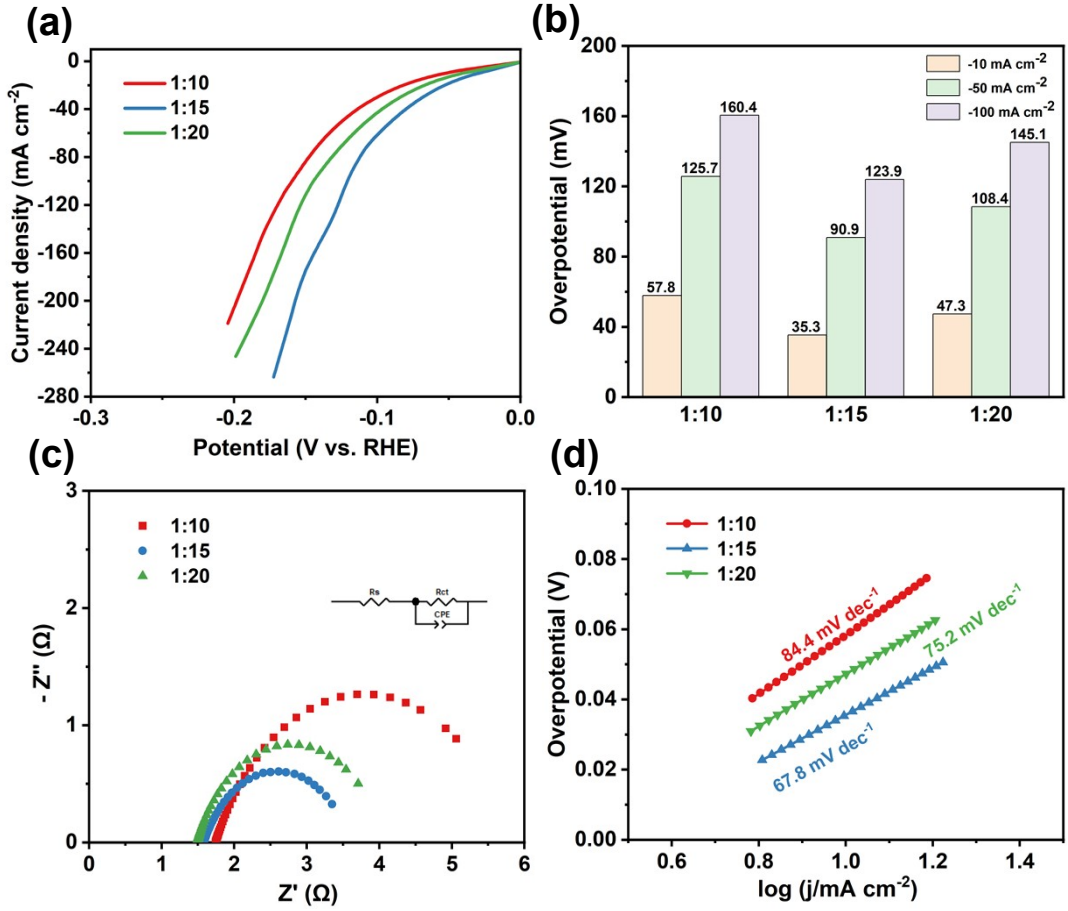

Fig. S6 HER performance of rGO/NiCoP fabricated with different GO/metal ratios in 1 M KOH: (a) LSV curve at a scan rate of 5 mV s^{-1}; (b) overpotential at current densities of -10, -50, and -100 mA cm^{-2}; (c) Nyquist plots; (d) corresponding Tafel plots.

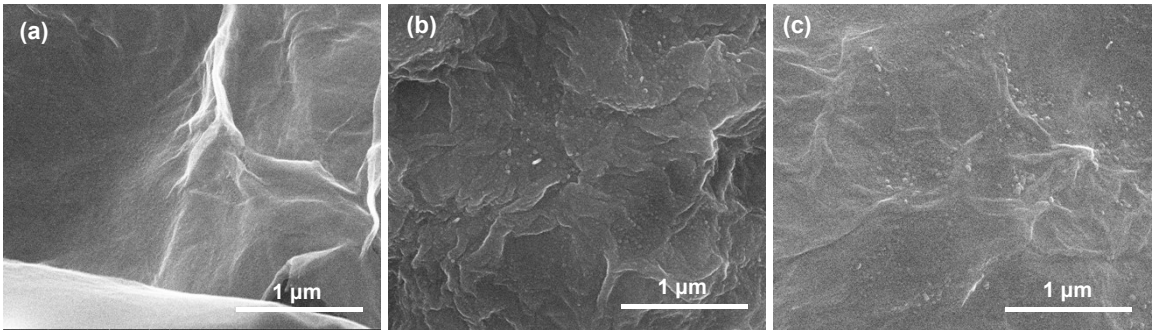

Fig. S7 rGO/NiCoP fabricated with different GO/metal ratios: (a) 1:10, (b) 1:15, (c) 1:20.

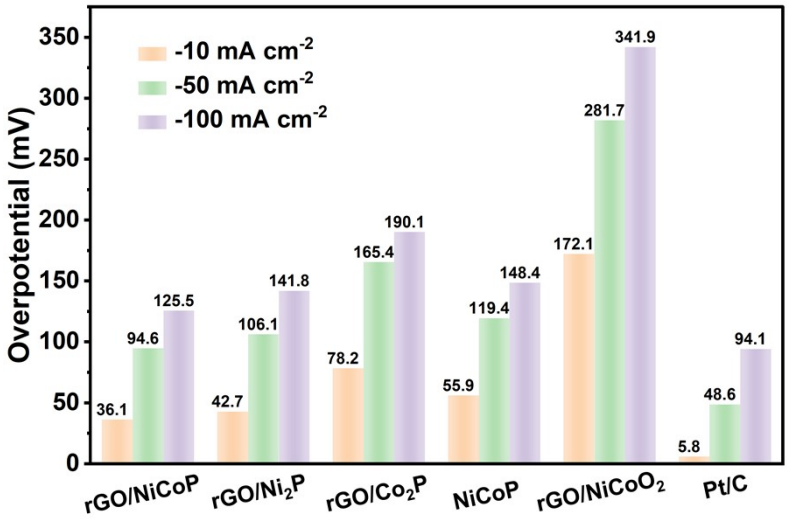

Fig. S8 Overpotentials at current densities of -10, -50, and -100 mA cm^{-2} for various catalysts in 1M KOH.

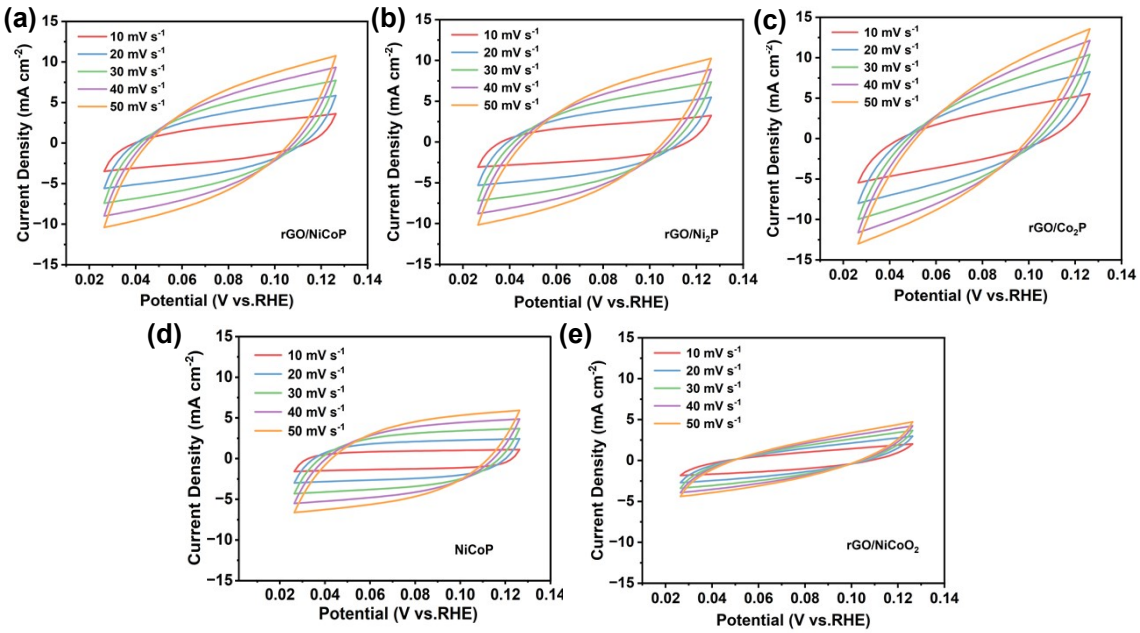

Fig. S9 CV curves of rGO/NiCoP, rGO/Ni_2P, rGO/Co_2P, NiCoP and rGO/$NiCoO_2$ at different scan rates.

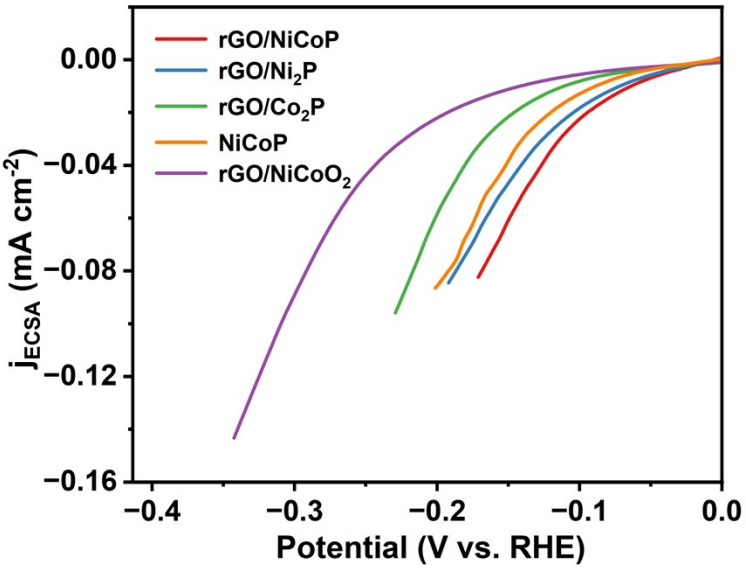

Fig. S10 ECSA-normalized LSV curves of rGO/NiCoP, rGO/Ni_2P, rGO/Co_2P, NiCoP and rGO/$NiCoO_2$.

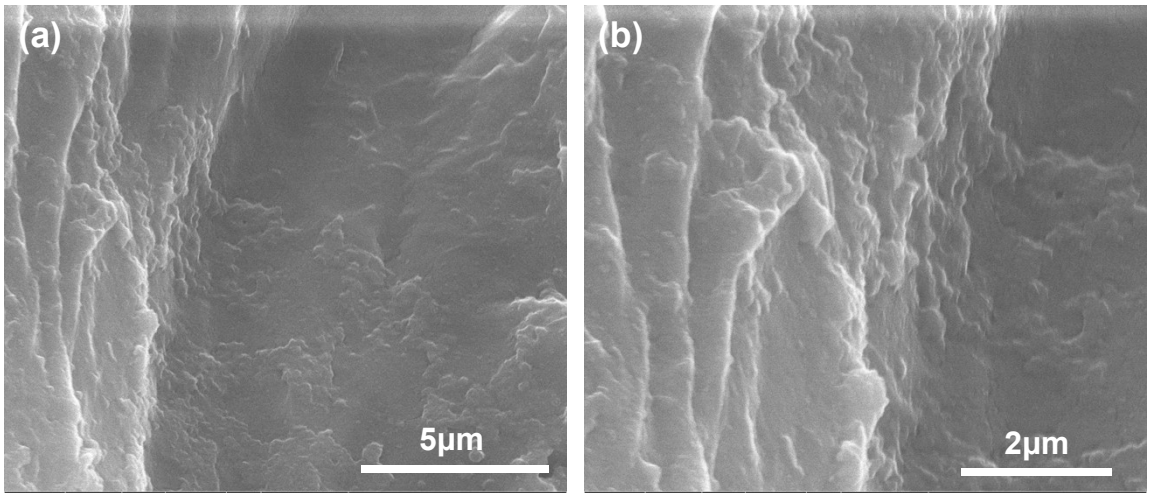

Fig. S11 SEM images of rGO/NiCoP after HER stability tests.

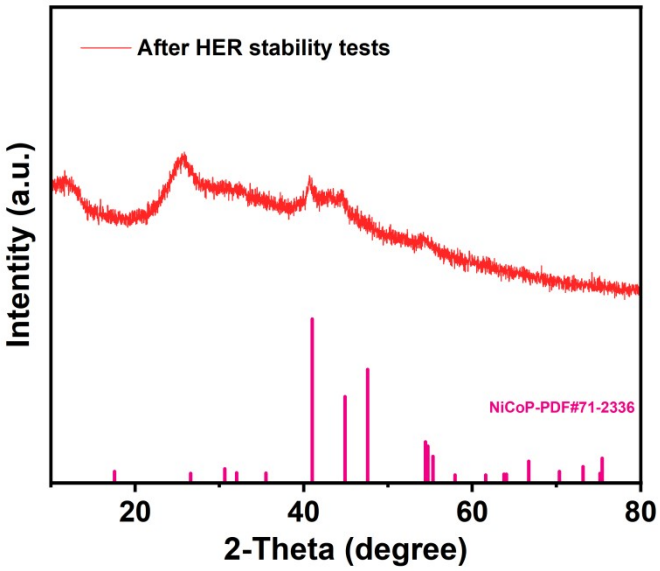

Fig. S12 XRD patterns of rGO/NiCoP after HER stability tests.

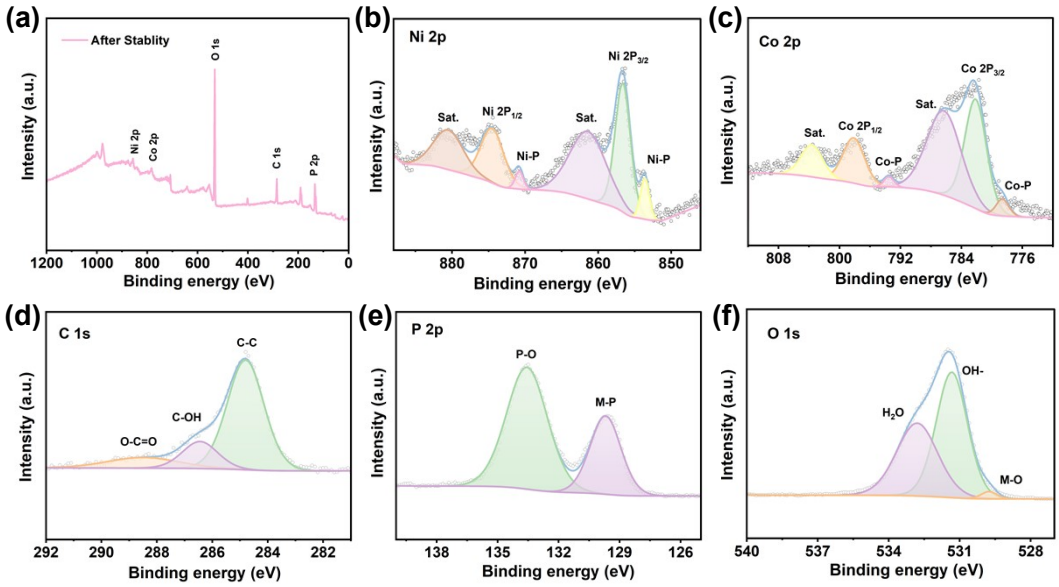

Fig. S13 XPS survey spectrum (a) and high-resolution spectrum of rGO/NiCoP after stability test: (b) Ni 2p, (c) Co 2p, (d) C 1s, (e) P 2p, and (d) O 1s.

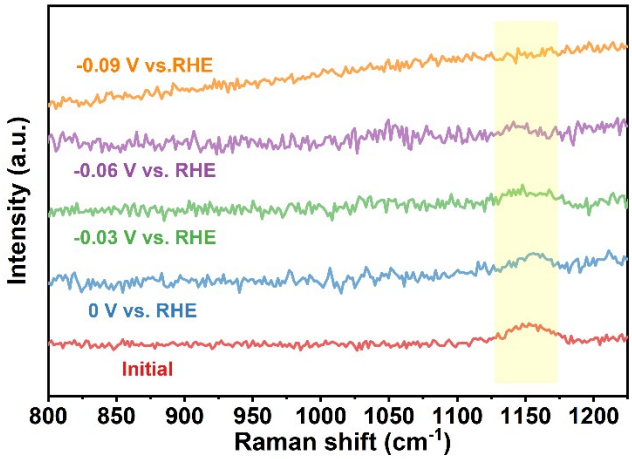

Fig. S14 In-situ Raman spectra of the rGO/NiCoP catalyst during HER.

Table S1. Comparison of HER performances of rGO/NiCoP with recently reported electrocatalysts in 1 M KOH.

Catalyst	η (mV) at -10 mA cm^{-2}	Tafel slope (mV/dec)	Reference
rGO/NiCoP	35.3	67.8	This work
Ru-Ni_2P@CoP	82.7	117.4	Ref. S1
NiCo/NiCoP	60	53.4	Ref. S2
e-CoNiFeP/NF	146	51.4	Ref. S3
MoP@N-NiCoP	43	45.9	Ref. S4
NiMoP/S-$Ti_3C_2T_x$@NF	121	46	Ref. S5
NiCoP/NiCo-LDH	84	121	Ref. S6
NiCoP	134.6	72.3	Ref. S7
FeOOH/NiCoP/NF	76	70.3	Ref. S8

Table S2. EIS fitting parameters for various catalysts.

	rGO/NiCoP	**rGO/Ni_2P**	**rGO/Co_2P**	**NiCoP**	**rGO/$NiCoO_2$**
R_s	1.85	1.79	1.82	1.65	2.54
R_{ct}	1.93	3.43	8.84	3.82	27.29

Table S3. C_{dl} value and corresponding ECSA of various catalysts.

Sample	**C_{dl} (mF cm^{-2})**	**ECSA**
rGO/NiCoP	101.1	2527.5
rGO/Ni_2P	97.0	2425.0
rGO/Co_2P	83.9	2097.5
NiCoP	87.7	2192.5
rGO/$NiCoO_2$	28.3	707.5

Table S4. Tafel value and exchange current density(j_0) of various catalysts.

Sample	**Tafel (mV dec^{-1})**	**j_0 (mA cm^{-2})**
rGO/NiCoP	68.6	2.86
rGO/Ni_2P	72.9	2.45
rGO/Co_2P	123.6	2.45

Table S5. Comparison of electrolysis performance of rGO/NiCoP with recently reported electrocatalysts in 1 M KOH.

Catalyst	Cell voltage [V] at 10 mA cm^{-2}	Reference
rGO/NiCoP	1.53	This work
NiCoP/NiCoP-LDH	1.64	Ref. S6
Al–CoNiP/NF	1.67	Ref. S9
Ce-NiCoP@C/NF	1.54	Ref. S10
NiFeP@Ni-NCNF	1.61	Ref. S11
m$Co_{0.5}Fe_{0.5}$P/rGO	1.66	Ref. S12
NiFeP NWs	1.68	Ref. S13
NiCuCoP	1.56	Ref. S14

References

1 X. Liu, H. Pang and X. Wu, *Chin. Chem. Lett.*, 2026, DOI: 10.1016/j.cclet.2025.111479.

2 X. Zhang, H. Xue, J. Sun, N. Guo, T. Song, J. Sun, Y.-R. Hao and Q. Wang, *Chin. Chem. Lett.*, 2024, **35**(2), 108519.

3 N. Zhang, J. Sun, J. Yu, Y. Xu, W. Liang, Y. Li, X. Gu, S. Hata, Z. Wu, Y. Wang and Y. Du, *J. Colloid Interface Sci.*, 2025, **698**, 138089.

4 Y. Zhang, X. Song, X. Guo and X. Li, *J. Colloid Interface Sci.*, 2023, **648**, 585-594.

5 D. Singh, M. Saquib and A.C. Bhosale, *Fuel*, 2026, **410**, 137921.

6 X. Guo, X. Bai and X. Wu, *Energy Fuels*, 2025, **39**(43), 20950-20956.

7 M. Ding, Q. Yu, Z. Wei and D. Liu, *Mater. Sci. Semicond. Process.,* 2025, **192**, 109461.

8 Y. Yuan, L.-B. Zhao and L.-H. Gan, *J. Environ. Chem. Eng.* 2025, **13**(3), 117220.

9 X. Su, X. Shao, J. Zhao, Z. Wang, C. Zhang, C. Song and D. Wang, *Int. J. Hydrogen Energy*, 2025, **105**, 638-645.

10 Y. Yuan, L.-H. Gan and L.-B. Zhao, *Inorg. Chem. Commun.*, 2025, **176**, 114328.

11 T. Huang, G. Xu, H. Ding, X. Liu and L. Zhang, *Sep. Purif. Technol.*, 2025, **354**，129094.

12 Y. Huang, F. Tian, Y. Liu, M. Li, S. Xu, Y. Yu, J. Li, W. Yang and H. Li, *J. Colloid*

Interface Sci., 2022, **605**, 667-673.
13 Y.-H. Chen, S. Kubendhiran, C.-H. Lin, L.-Y. Lin and K.-C. Ho, J. Colloid Interface Sci., 2026, 716, 140301.
14. A. Talebi, G.B. Darband, M. Mirjalili and J. Li, *J. Mater. Chem. A* 2026, **14**, 8895.